Supplementary Information for:

Can molecular flexibility control crystallization? The case of para substituted benzoic acids

Sin Kim Tang, Roger J. Davey*, Pietro Sacchi and Aurora J. Cruz-Cabeza

S1 Conformational analysis.

Methods

Cambridge Structural Database (CSD). The Cambridge Structural Database[1] (2018 release) was used together with the CSD systems software Mercury[2] and Mogul[3]. The CSD was searched using Conquest to retrieve the crystal structure of *p*BOBA (BUXBZA01[4]). The crystal structure of pPENTYLBA was determined as part of this work and deposited in the CSD as CCDC Deposition 2003448. The visualiser Mercury was used to overlay the conformations found in the *p*BOBA and *p*PENTYLBA crystal structures.

MOGUL Conformational Analysis. Mogul[3] was used to derive conformational preferences (torsions) in related compounds from the CSD. For this, a conformation of the molecule of interest (*p*BOBA and *p*PENTYLBA) was selected and a MOGUL analysis performed via the CSD visualiser Mercury[2]. For the Mogul analysis, the following filters were applied: i) crystal structures had to have an R factor of less than 5%, ii) structures with solvent, organometallics and structures solved from powders were not allowed and iii) the standard settings for fragment similarities was used.

Generation of Potential Energy Surfaces (PESs). The linear CL conformations of *p*BOBA and *p*PENTYLBA were generated using Avogadro[5,6] and taken forward for DFT minimisation in Gaussian09[7]. The M06[8] functional was used together with the 6-31+G** basis set for geometry optimisation in the gas-phase. Starting from the linear conformations, the potential energy surface as a function of θ_1, θ_2, θ_3 and θ_4 were explored independently. The PES was generated as a function of each of the torsion angles by performing redundant optimisations by constraining the explored torsion to values from 0° to 180° in steps of 5^0. The 180° to 360° PES energies were generated by mirroring the 0° to 180° values. After all PES were performed, the lowest calculated conformational energy was taken as reference and thus all the conformational energies are given relative to the most stable conformer. PESs were then also generated toluene and IPA making use of an SMD solvation model[9] and using the same procedure described for the gas-phase.

Table S1.1: Torsion angles of conformations in *p*BOBA (Refcode: BUXBZA01) and *p*PENTYLBA (CCDC Deposition number 2003448).

		Selected Torsion Angles, θ / °			
Conformation	***Conformer***	θ_1	θ_2	θ_3	θ_4
BUXBZA01 m1	CL	179.69	179.80	-176.48	178.44
BUXBZA01 m1-inverted	CL-i	-179.69	-179.80	176.48	-178.44
BUXBZA01 m2	CT	3.59	174.62	-63.34	-175.15
BUXBZA01 m2-inverted	CT-i	-3.59	-174.62	63.34	175.15
Gas-Optimal m1	CL	180/0	180	180	180
Gas-Optimal m1-inverted	CL-i	180/0	180	180	180
Gas-Optimal m2	CT	180/0	180	-60	180
Gas-Optimal m2-inverted	CT-i	180/0	180	60	180
Form I m1	CTa	85.73	178.27	-73.85	179.33
Form I m1-inverted	CTa-i	-85.73	-178.27	73.85	-179.33
Form I m2	CTa	74.32	176.23	-65.34	-176.76
Form I m2-inverted	CTa-i	-74.32	-176.23	65.34	176.76
Form I m3	CTb	116.84	173.96	70.25	166.31
Form I m3-inverted	CTb-i	-116.84	-173.96		
Gas-Optimal m1/2	CTa	90	180	-60	180
Gas-Optimal m1/2-inverted	CTa-i	-90	180	60	180
Gas-Optimal m3	CTb	90	180	60	180
Gas-Optimal m3-inverted	CTb-i	-90	180	-60	180

Figure S1.1 Mogul results and PES for *p*PENTYL and *p*BOBA.

*p*PENTYLBA

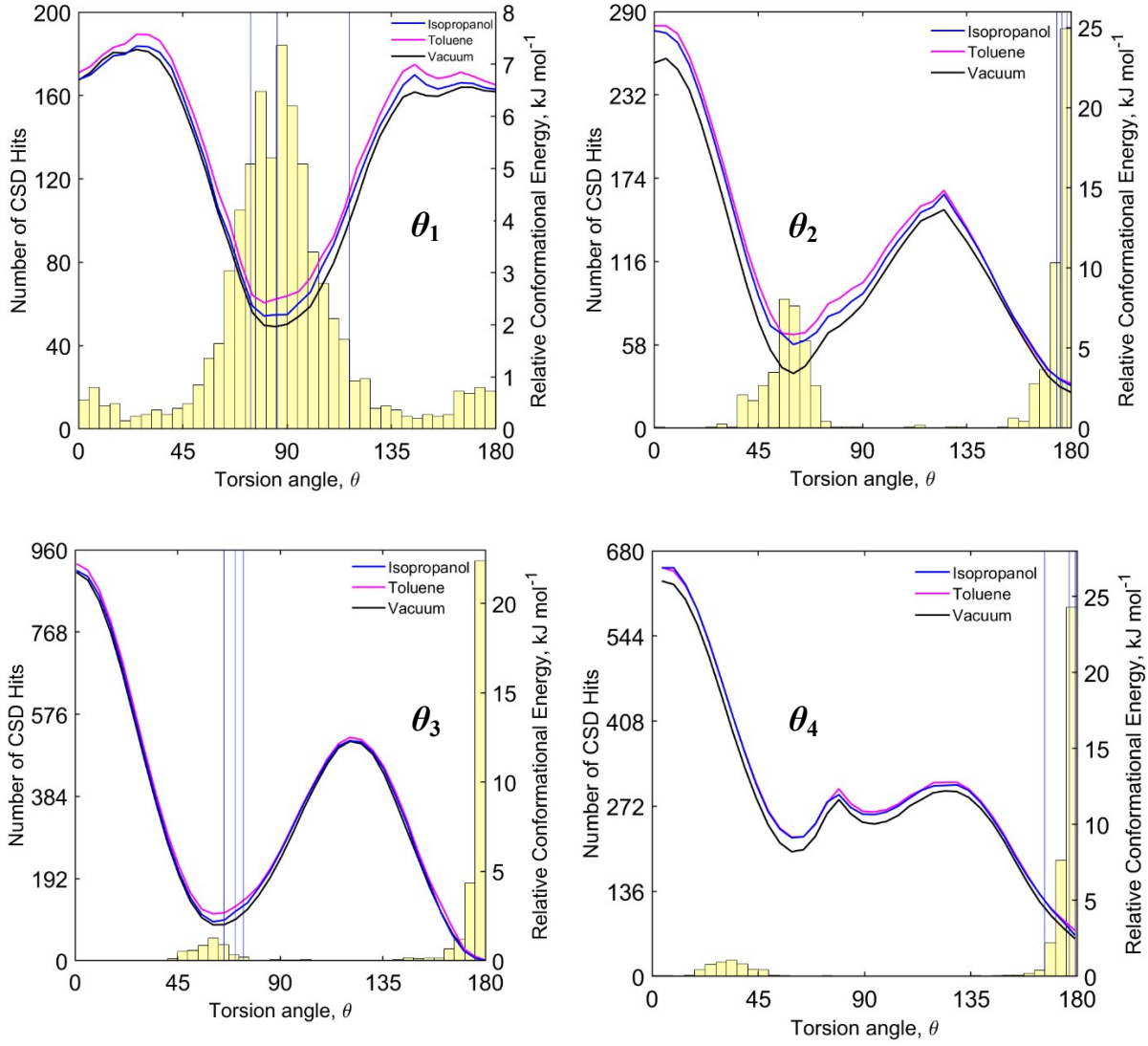

*p*BOBA

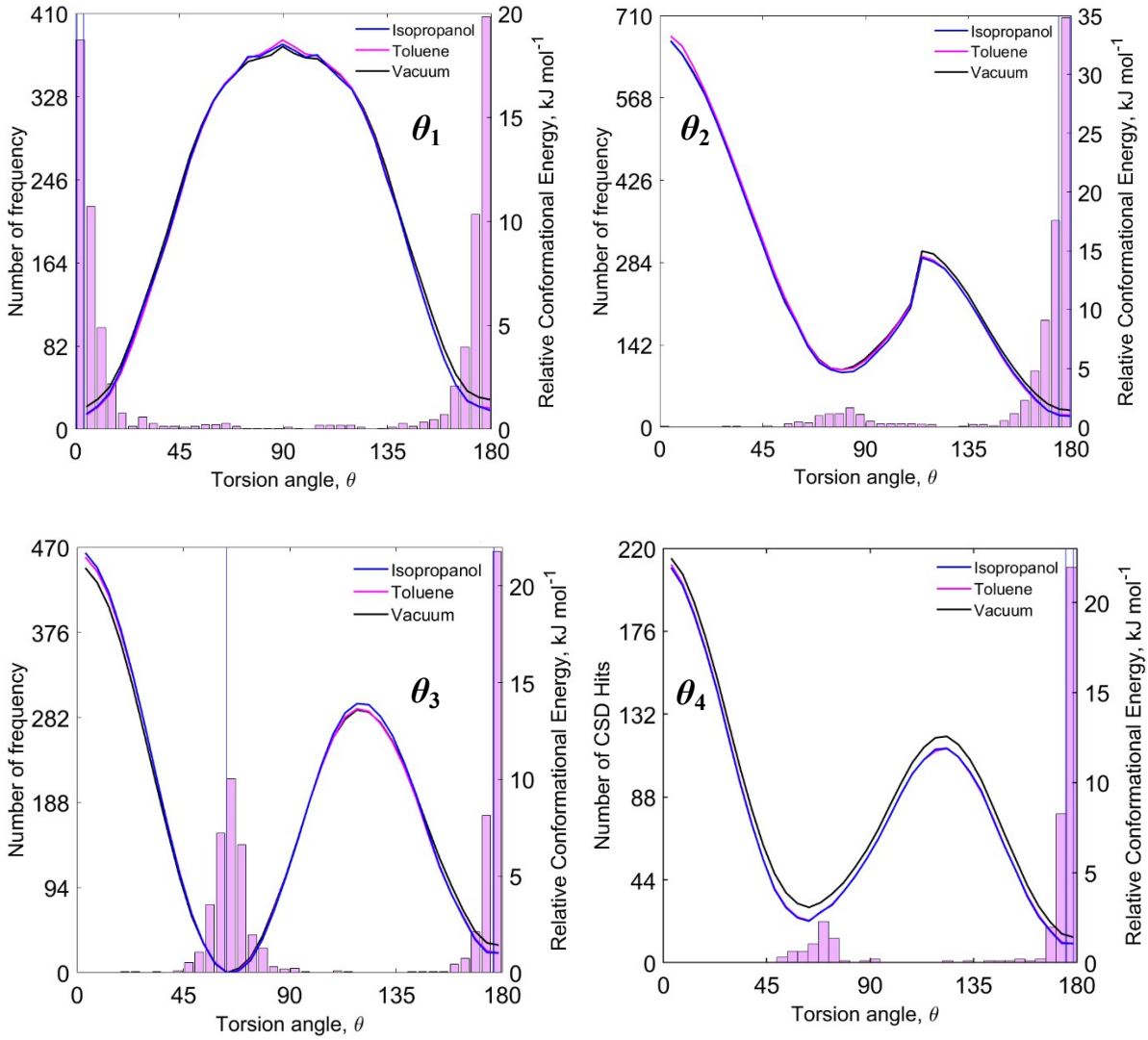
Isopropanol
Toluene
Vacuum
θ_1
θ_2
θ_3
θ_4
Number of frequency
Number of CSD Hits
Relative Conformational Energy, kJ mol^{-1}
Torsion angle, θ

Figure S1.2. Gas potential energy surface for *p*BOBA (upper) and *p*PENTYLBA (lower) upon rotation of θ_3 in the gas-phase (blue) as well as in toluene and IPA (orange and grey respectively). The conformational preferences in the CSD for related molecules is also shown (bar-plot) together with the values observed in the crystal conformations CTa, CT and CT-i (grey bars) and CTb, CL and CLi (blue bars). The conformations of the chain are shown for illustration with the aromatic carbon indicated with an orange circle and the hydrogen atoms hidden.

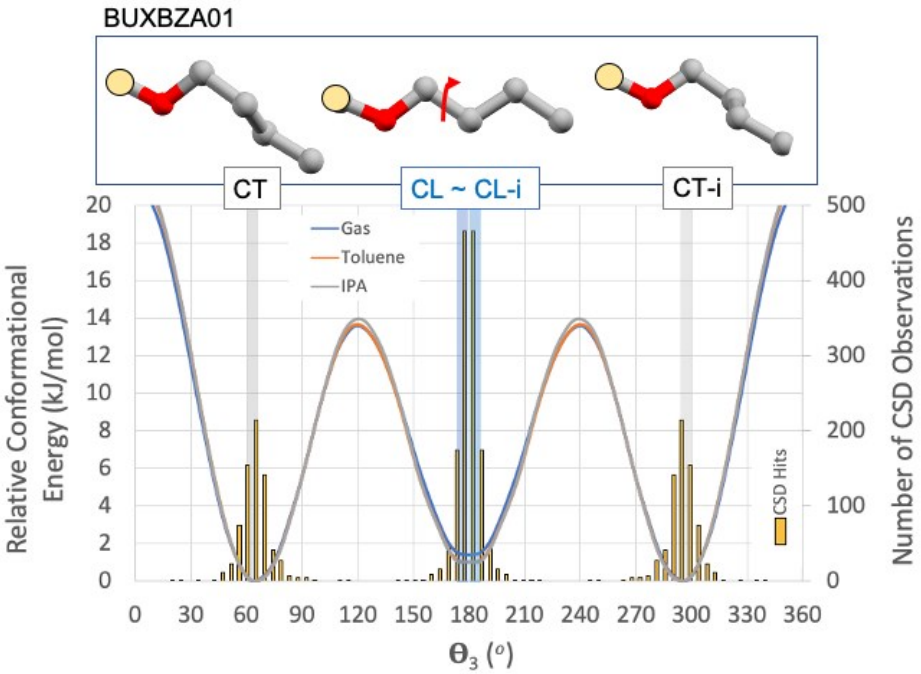

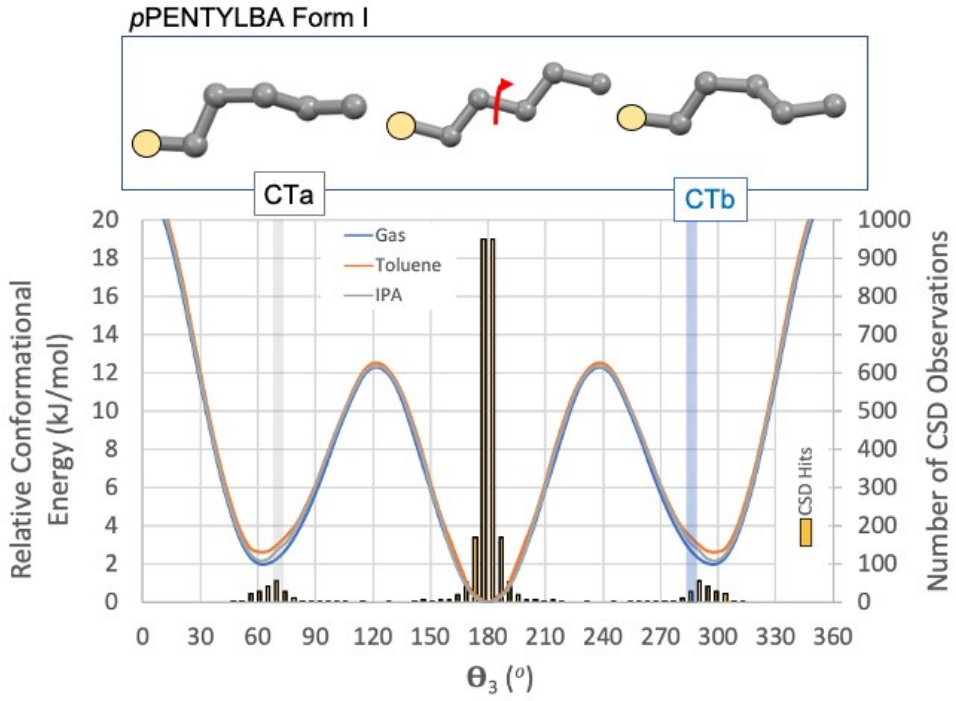

S2. Solubility and Thermal analysis.

Solubilities were determined gravimetrically.

Table S2.1 Solubility of *p*BOBA and *p*PENTYLBA in toluene and IPA at various temperatures.

Solute in solvent	Temperature / ^{0}C	Solubility / $kg_{solute}\ kg_{solvent}^{-1}$		Mole fraction / -		Molarity / mol m^{-3}	
*p*BOBA in TOL	10.0	0.0061	± 0.0003	0.0029	± 0.0002	27.2062	± 1.4547
	20.0	0.0103	± 0.0001	0.0049	± 0.0001	45.5826	± 0.5519
	30.0	0.0190	± 0.0002	0.0089	± 0.0001	83.1627	± 0.9938
	40.0	0.0326	± 0.0006	0.0152	± 0.0003	140.7004	± 2.5276
*p*BOBA in IPA	10.0	0.0252	± 0.0002	0.0077	± 0.0001	99.4392	± 0.6946
	20.0	0.0397	± 0.0004	0.0121	± 0.0001	153.5874	± 1.6394
	30.0	0.0616	± 0.0005	0.0187	± 0.0002	234.6476	± 2.1881
	40.0	0.0971	± 0.0007	0.0292	± 0.0002	358.0662	± 2.6433
*p*PENTYLBA in TOL	10.0	0.2363	± 0.0020	0.1017	± 0.0010	862.0177	± 9.1743
	20.0	0.4140	± 0.0007	0.1656	± 0.0003	1320.2721	± 3.2475
	30.0	0.5381	± 0.0088	0.2050	± 0.0042	1577.4536	± 39.4480

Table S2.2 DSC data for 4 benzoic acids. * see references 4 and 10 for literature values.

S3 Nucleation kinetic data.

S3.1 Typical Induction Time probability Distributions.

Figure S3.1: Experimentally measured cumulative probabilities distribution, P_{exp} of detection times (colour circles) and fitted curves $P(t_D)$ for *p*BOBA and *p*PENTYLBA in different solvents over a range of supersaturation, S (categorised under different colour as indicated in the legend accordingly). (a) *p*BOBA in TOL at 20^{0}C, (b) *p*BOBA in IPA at 20 ^{0}C, (c) *p*PENTYLBA in TOL at 20 ^{0}C and (d) *p*BOBA in TOL at 40 ^{0}C and the coloured shadings refers to their resulting 95% confidence intervals within the probability distribution curves.

Sample	Thermal Event Information	Peak Temperature, °C	Latent Heat, kJ mol^{-1}
BA	(1) Melting	(1) 125.8	(1) 17.6
PTA	(1) Melting (2) Decomposition	(1) 183.7 (2) 239.6	(1) 16.1 (2) 26.5
*p*BOBA*	(1) Nematic liquid (2) Isotropic melt	(1) 149.3 (2) 161.8	(1) 19.1 (2) 2.9
*p*PENTYLBA*	(1) Nematic liquid (2) Isotropic melt	(1) 88.9 (2) 127.5	(1) 11.4 (2) 1.8

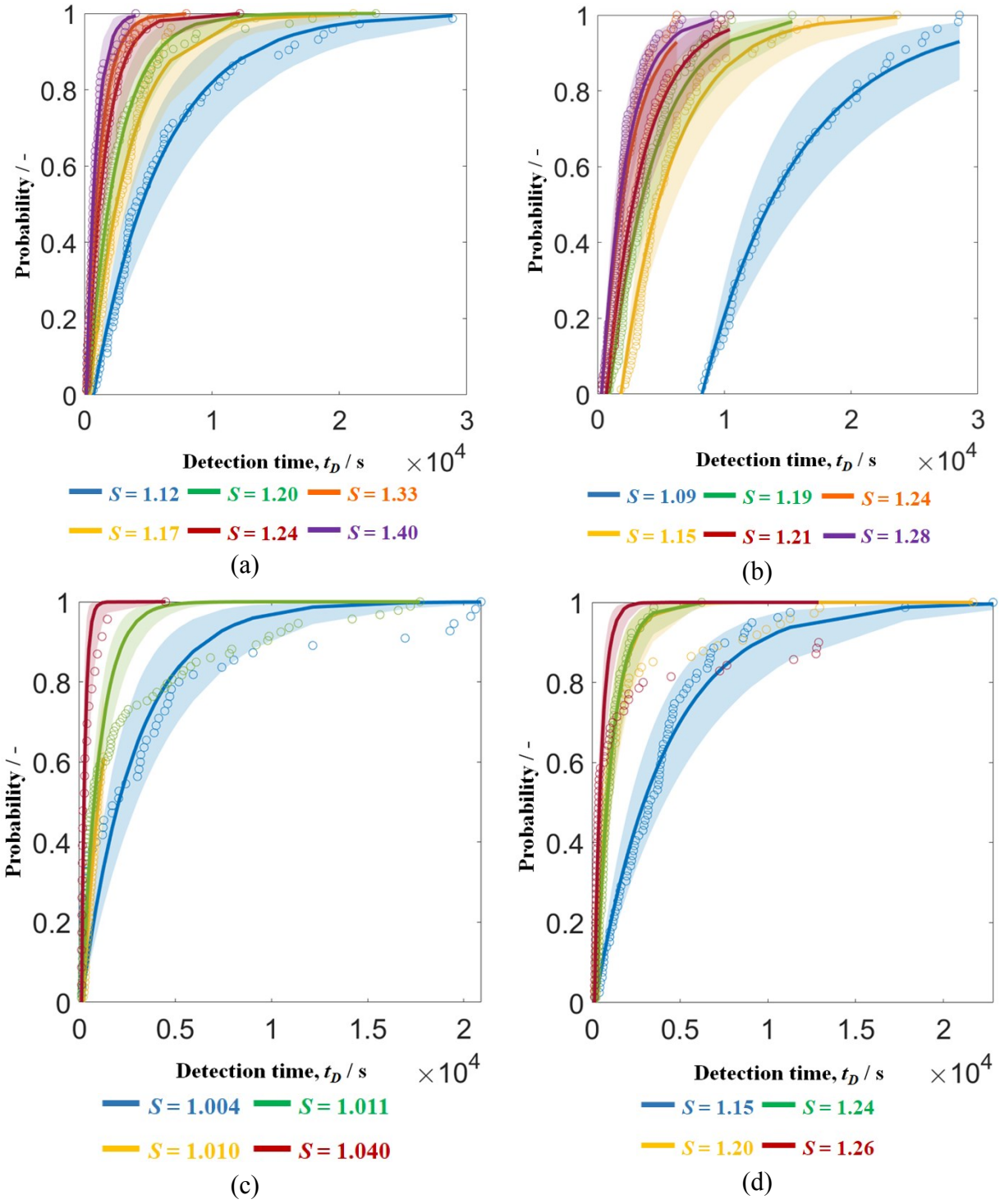

S3.2 Nucleation rates and fitted parameters.

Table S3.1 ***para*-butoxybenzoic acid (*p*BOBA) experimental nucleation rates, J with 95% confidence intervals, growth time, t_g, number of experiments where nucleation was detected, N_{nuc} over a range of supersaturations, S in different solvents at 20 °C and 40 °C.**

Toluene (TOL) T = 20 °C	Toluene (TOL) T = 40 °C	Isopropanol (IPA) T = 20 °C

S	J / m^{-3} s^{-1}		N_{nuc}	t_g / s	S	J / m^{-3} s^{-1}		N_{nuc}	t_g / s	S	J / m^{-3} s^{-1}		N_{nuc}	t_g / s
1.12	122	85 – 179	73	700	1.15	166	116 - 235	74	160	1.09	87	58 - 132	55	8235
1.17	219	151 - 311	80	400	1.20	694	466 - 1013	74	145	1.15	160	112 - 228	79	1853
1.20	279	193 - 397	75	240	1.24	740	515 - 1053	78	195	1.19	187	131 - 266	80	920
1.24	456	315 - 669	73	135	1.26	1626	1070 - 2453	70	125	1.21	223	156 - 317	59	685
1.33	609	428 - 860	77	120						1.24	297	209 - 423	80	320
1.40	886	586 - 1346	61	135						1.28	334	233 - 476	70	315

Table S3.2: *para*-pentylbenzoic acid (*p*PENTYLBA) experimental nucleation rates, J with 95% confidence intervals, growth time, t_g, number of experiments where nucleation was detected, N_{nuc} over a range of supersaturations, S in toluene at 20 ^{0}C.

Toluene (TOL) T = 20 °C				
S	J / m^{-3} s^{-1}		N_{nuc}	t_g / s
1.0036	240	160 - 362	58	135
1.0099	586	368 - 924	60	215
1.0106	701	499 - 980	110	125
1.0401	3746	1781 - 7883	23	130

Nucleation rate – supersaturation data was fitted to the CNT equation (Equation 1 in the main paper). While nucleation mechanisms from solution remain a matter of debate this equation is commonly used and yields values of the rate constant A and the thermodynamic factor B which are given by the following expressions:

$$A = \frac{f_0 C_0}{\sqrt{12\pi B}}$$

$$B = \frac{16\pi \vartheta_0^2 \gamma^3}{3k_b^3 T^3}$$

In which, ϑ_0 is the volume of a solute molecule, γ is the interfacial free energy between the nucleus surface and solution, k_B is the Boltzmann constant, T is the temperature, f_0 is the

supersaturation independent part of the attachment frequency and C_0 is the equilibrium concentration of nuclei[11].

Figure S3.2 The nucleation rates *J*, of *p*BOBA and *p*PENTYLBA versus supersaturation, *S* at 20^{0}C. (a) *p*BOBA in toluene, (b) *p*BOBA in IPA, (c) *p*PENTYLBA in toluene, (d) *p*BOBA in toluene at 20 °C (open circle) and 40 °C (filled circles). Open circles refer to experimental data points with vertical solid lines showing 95% confidence intervals. Fitted curves represent the re-calculated nucleation rates using CNT equation (equation 1): solid lines derived from linear and dotted from non-linear fitting.

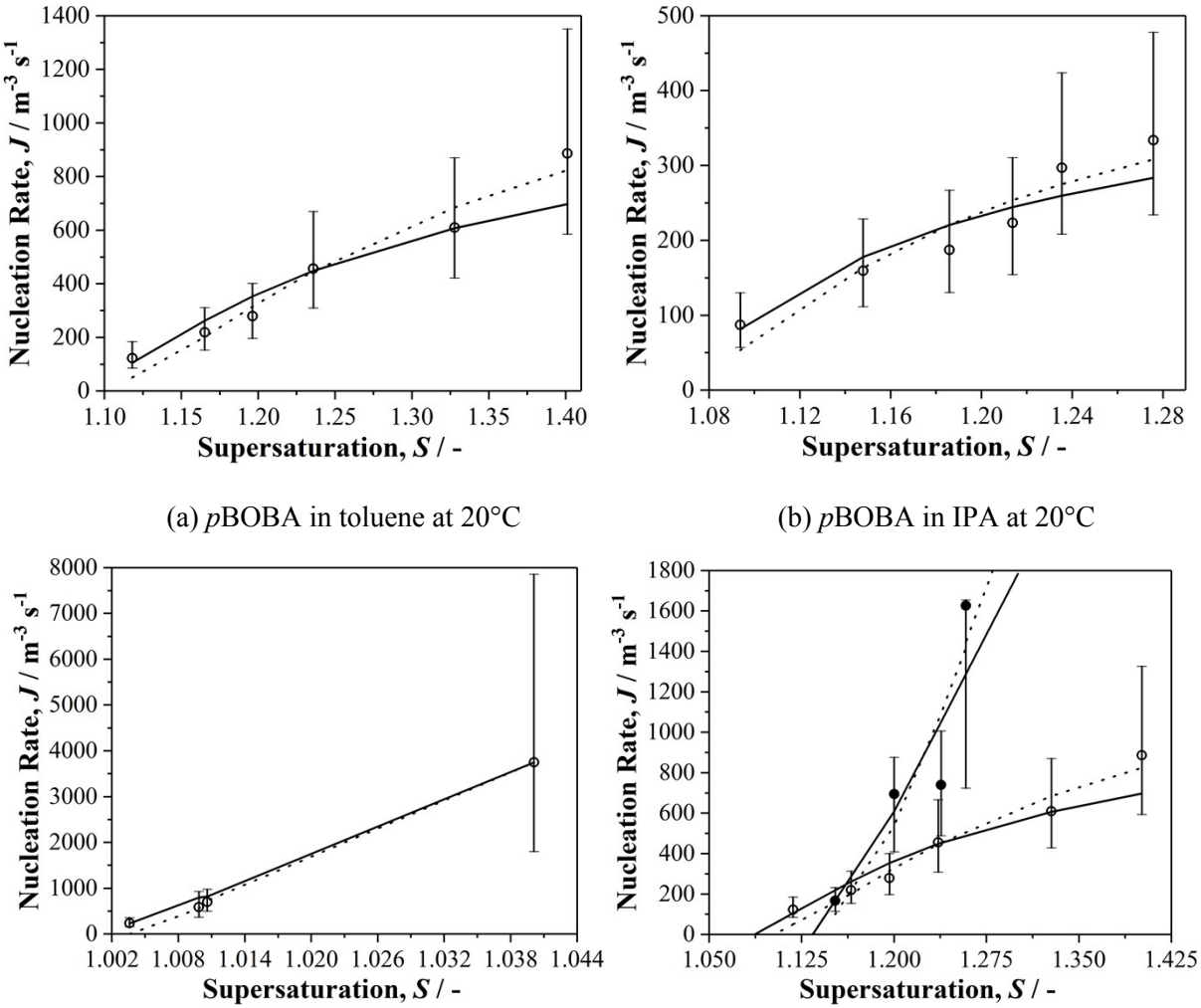

(a) *p*BOBA in toluene at 20°C

(b) *p*BOBA in IPA at 20°C

(c) *p*PENTYLBA in toluene at 20°C

(d) *p*BOBA in toluene at 20°C & 40°C

Figure S3.3: Plot of ln ($J\ S^{-1}$) against 1/ ($\ln^2 S$) for (a) *p*BOBA in different solvents at 20 °C (squares) and 40 °C (crosses) and (b) *p*PENTYLBA in toluene at 20 °C (diamonds). Note that squares and diamonds represent *p*BOBA and *p*PENTYLBA respectively. As for the solvent representation, the filled and open symbols refer to toluene and isopropanol.

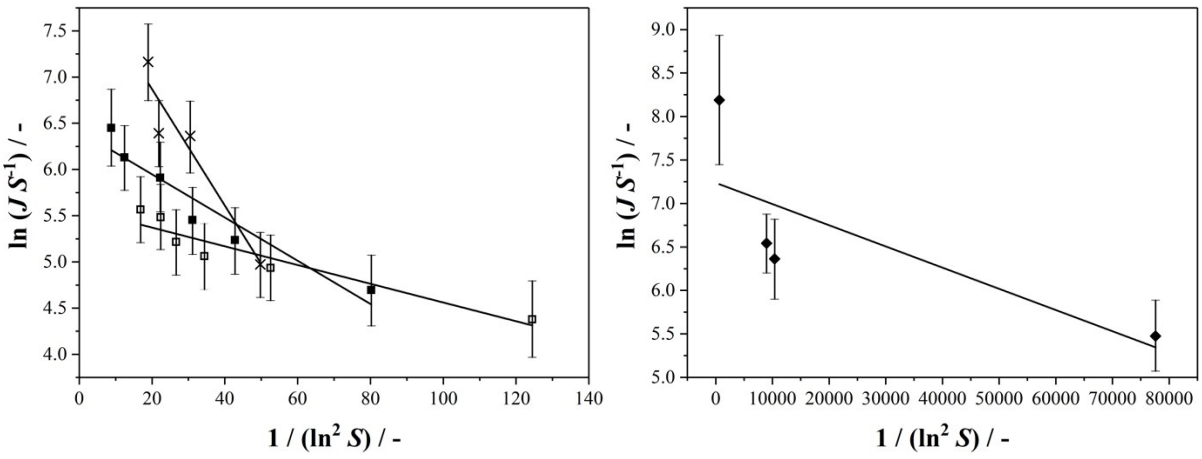

Figure S3.4: Plots of ln (*J* / *S*.M) against 1/ (ln^2 *S*) for (a) *p*BOBA in different solvents at 20 °C (squares) and 40 °C (crosses) and (b) *p*PENTYLBA in toluene at 20 ^{0}C (diamonds). As for the solvent representation, the filled and open symbols refer to toluene and isopropanol.

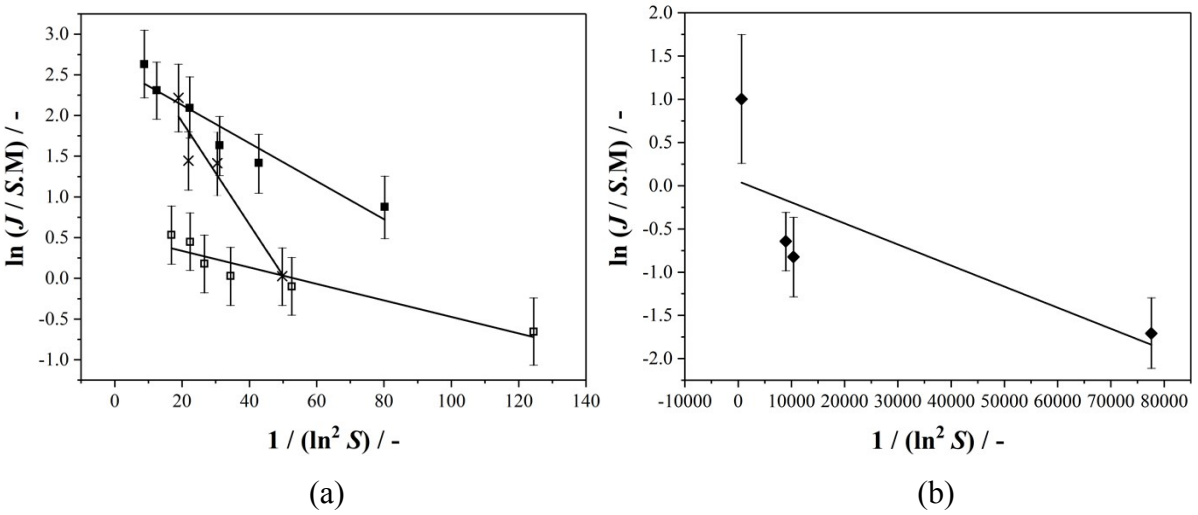

Table S3.3 Nucleation parameters for BA, *p*TA, *p*BOBA and *p*PENTYL derived using the interface-transfer controlled nucleation Equation 1, using linear fitting. *data taken from references 12 and 13.

Solute	**Solvent**	***A* x 10^{-2} / m^{-3} s^{-1}**	***B* x 10 / -**	***γ* / mJ m^{-2}**	***A'* / mol^{-1} s^{-1}**

BA*	TOL	11.46 (10.29 - 14.18)	4.95 (4.86 - 5.36)	8.29 (8.16 - 8.43)	2.03 (1.82 - 2.51)
BA*	IPA/W	2.02 (1.13 - 2.79)	4.57 (4.27 - 4.89)	8.00 (7.82 - 8.18)	0.36 (0.20 - 0.50)
*p*TA*	TOL	30.41 (22.99 - 35.09)	0.33 (0.31 - 0.34)	2.72 (2.67 - 2.77)	38.27 (28.92 - 44.15)
*p*TA*	IPA	19.76 (13.29 - 29.23)	0.94 (0.92 - 0.96)	3.88 (3.86 – 3.92)	3.15 (2.38 - 5.16)
*p*BOBA	TOL	6.12 (4.10 - 8.68)	0.232 (0.230 - 0.233)	1.963 (1.959 - 1.966)	13.42 (9.00 – 19.05)
*p*BOBA	IPA	2.64 (1.87 - 3.73)	0.101 (0.099 - 0.108)	1.50 (1.48 - 1.52)	1.72 (1.22 - 2.43)
*p*PENTYLBA	TOL	9.53 (6.22 - 14.73)	1.85×10^{-4} $(1.80 \times 10^{-4} - 1.89 \times 10^{-3})$	0.172 (0.170 - 0.0887)	1.05 (0.47 - 1.12)
*p*BOBA ($T = 40\ ^0$C)	TOL	31.74 (20.81 - 47.56)	0.618 (0.606 - 0.630)	2.82 (2.80 - 2.84)	24.11 (14.79 - 33.80)

Figure S3.5 Correlations between ln (*A*) and (a) solubility: mole fraction, (b) solubility: molarity, (c) standard molar dissolution enthalpy changes estimated from solubility data, (d) solvent dielectric constant and (e) surface tension γ vs ln mole fraction solubility x_{sat}. Symbols: circles, stars, squares and diamonds represent BA, *p*TA, *p*BOBA and *p*PENTYLBA respectively. Black, white and white dashed filled symbols refer to toluene, isopropanol and acetonitrile.

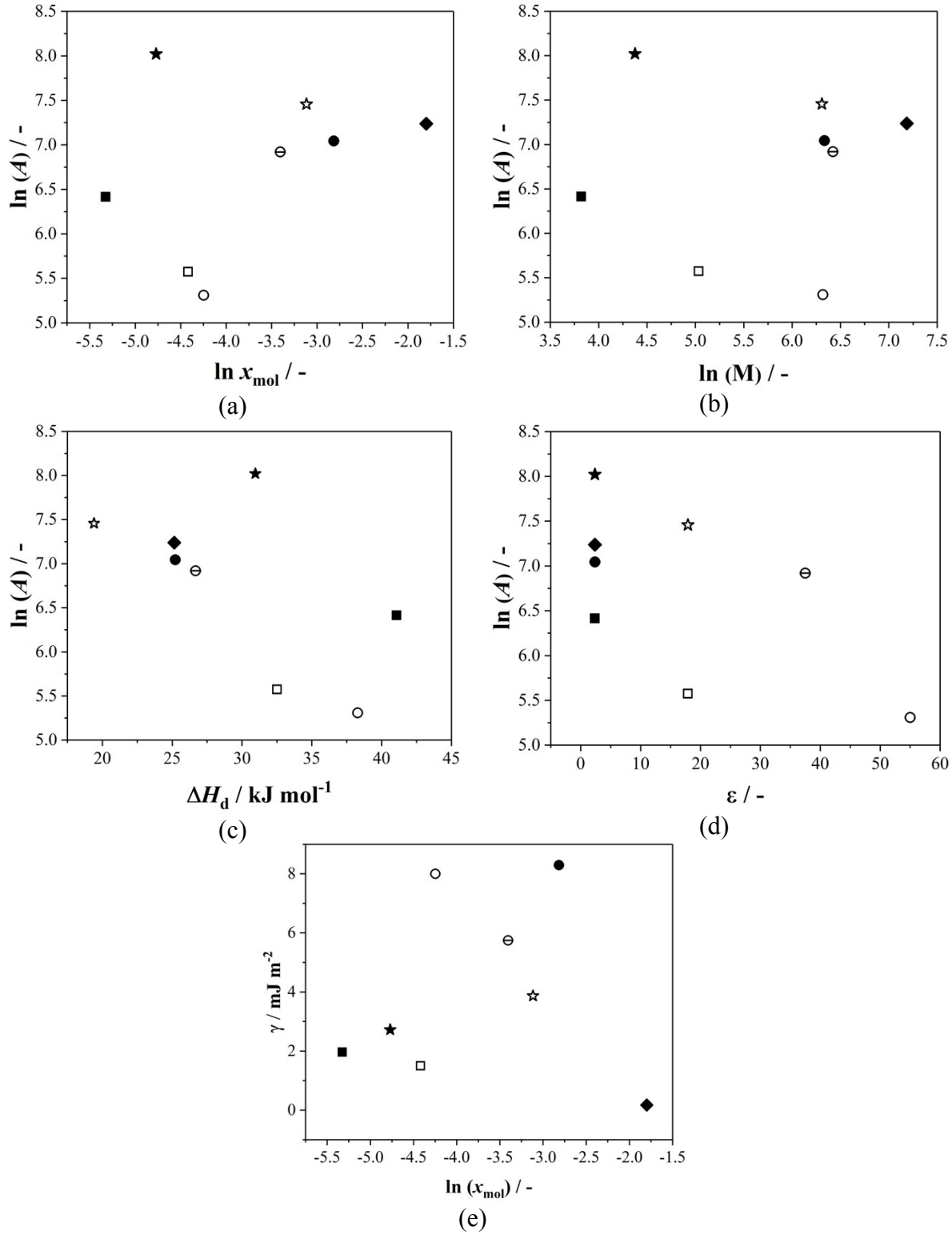

Figure S3.6 Plot of J M^{-1} vs S demonstrating the estimation of S_1 (value of S for which J/M = 1) (a) *p*PENTYLBA, *p*TA, *p*BOBA and BA in TOL, and (b) in IPA. Solid lines from linear fitting of CNT. Circles, stars, squares and diamonds symbols represent BA, *p*TA, *p*BOBA and *p*PENTYLBA respectively. As for the solvent representation, the filled and open symbols refer to toluene and isopropanol. Note that the dotted line in (a) refers to *p*BOBA in TOL. For BA in IPA (b) The dashed and solid lines show the estimated values of S_1 based on non-linear and linear fits respectively.

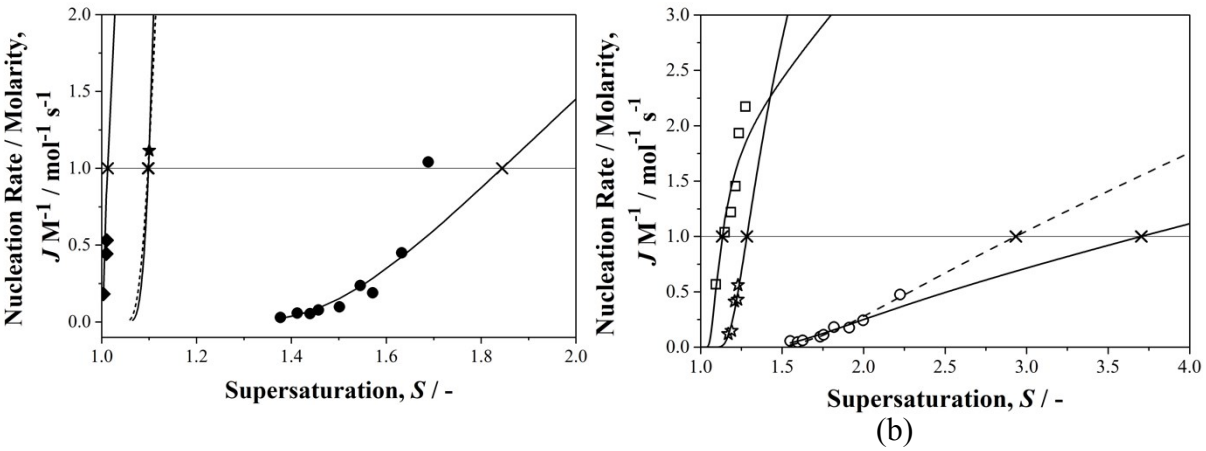

(a) (b)

S4 Analysis of principal intermolecular interactions and calculation of dimer energies

S4.1 Crystal structure of pBOBA (BUXBZA01)[4]

The crystal structure of pBOBA is formed of layers parallel to the *ac* plane (Figure S4.1a). which are connected by hydrogen bonds between the carboxylic acid groups of identical conformers oriented along the [01-1] direction. Within each layer two main types of secondary interactions can be identified: stacking interactions between inversion-related molecules involving the aromatic rings and the butoxy chains (labelled as St1 and St2 in Figure 4.1b and shown in more detail in Figure S4.1c) and t-type interactions between symmetry independent conformers (labelled as T1 and T2 in Figure S4.1b).

Figure S4.1 a) 2D layers parallel to the *ac* plane in pBOBA; b) principal secondary interactions within each layer as described in the text; c) detail of the stacking interactions St1 and St2. Different colours identify different conformers.

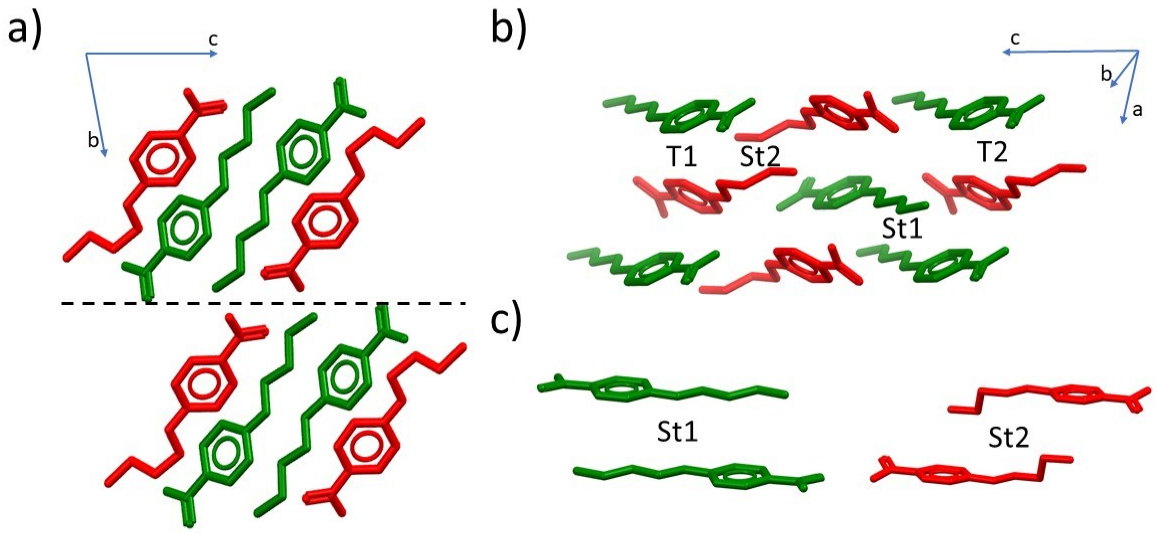

S4.2 Crystal structure of pPENTYLBA (CCDC Deposition 2003448)

The crystal packing of pPENTYLBA is more complicated due to the presence of three symmetry independent conformers (Z'=3). A convenient way of visualising the structure is by considering two-dimensional layers of molecules parallel to the (-121) plane (Figure S4.2a and S4.2b). Adjacent layers are connected by weak contacts, and all of the principal interactions found in the crystal structure lie within these layers (Figure S4.2c). For example, hydrogen bonds between carboxylic acid groups and aromatic stacking interactions of varying nature: ring-ring stacking (labelled St1 in Figure S4.2c), chain-ring stacking with involvement of the carboxylic acid group (labelled St2 and St3 in Figure S4.2c) and chain-ring stacking (labelled St4).

Figure S4.2 a) 2D layers parallel to the (-121) plane in pPENTYLBA: b) the same 2D layers after rotation of 90° and c) the principal intermolecular interactions present in the structure. Different colours identify different conformers.

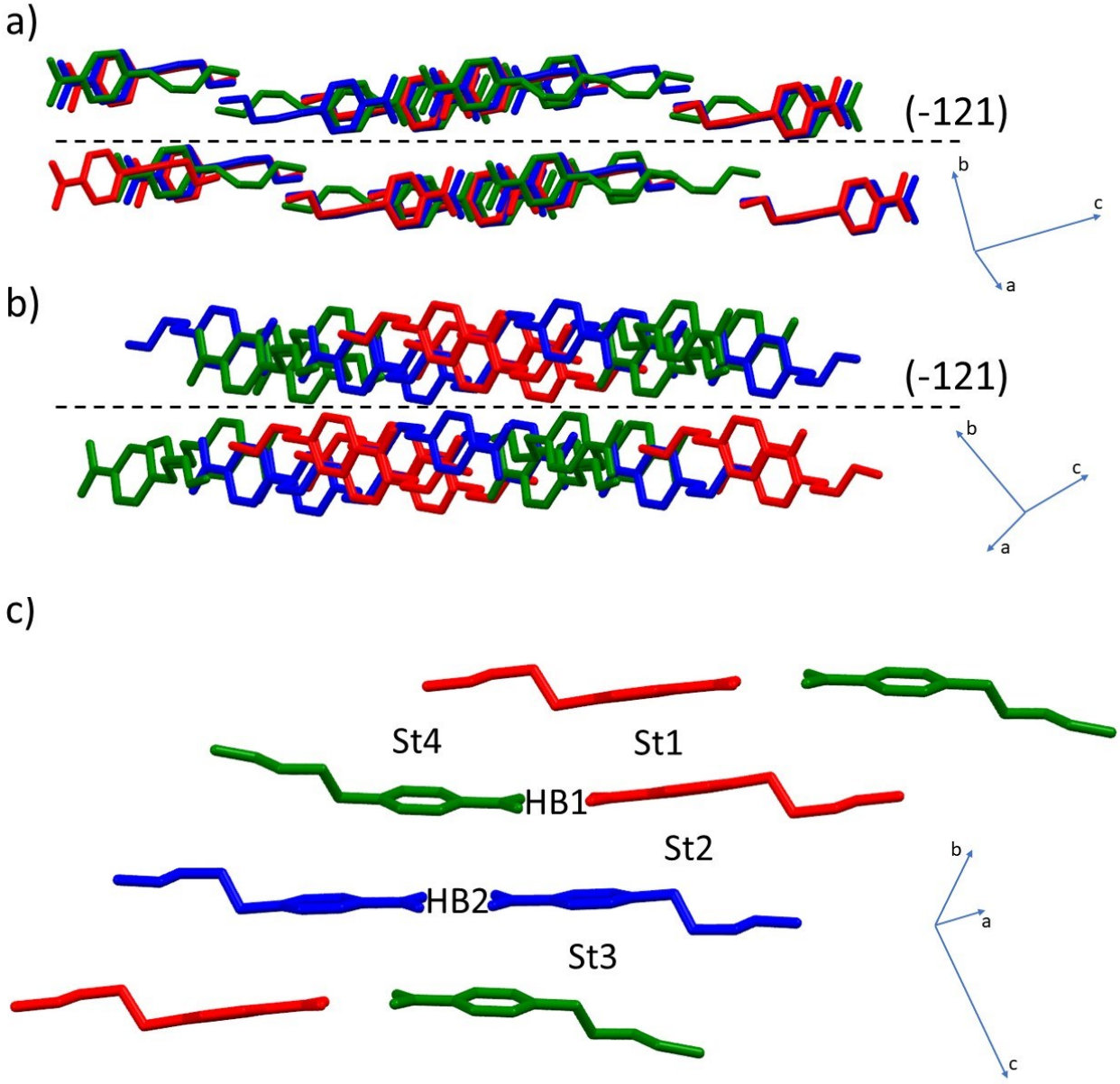
a)
(-121)
b
c
a
b)
(-121)
b
c
a
c)
St4
St1
HB1
St2
HB2
St3
b
a
c

S.4.3 Calculation of dimer energies

Dimer interaction energies (St1-4 for *p*PENTYLBA; St1 and2 and and T1 and T2 for *p*BOBA) were calculated with DFT-d using VASP 5.4.4[14-17] re-compiled with the VASPsol module[16] using the PBE functional[18] with PAW pseudopotentials[19,20] and applying Grimme's GD2 dispersion correction[21]. Crystal structures were first optimised relaxing both cell parameters and atomic positions, and then re-optimised relaxing atomic positions only. The dimers corresponding to the interactions described in Sections S4.1 and S4.2 above were then extracted from the optimised structures and put in simulation cells of 30x30x30Å. Isolated molecules were also simulated using an identical cell. The difference between the electronic energies of each dimer and its two isolated molecules resulted in intermolecular dimer energies, while the difference between the electronic energy of the crystal and of one molecule isolated in the gas-phase was used to calculate the lattice energy, E_{latt}. Calculated energies of the principal dimers in *p*BOBA and *p*PENTYLBA calculated in implicit solvation models[22,23] for toluene and IPA are reported in table S4.1 below, together with the interaction energies calculated for BA and pTA in a previous work[13].

Table S4.1 Interaciton energies calculated by DFT-d for the principal dimers of pBOBA, pPENTYLBA, pBA and pTA. The latter two, identified with * in the table, were calculated in a previous work[14].

	Solute	**Toluene** (ε = 2.37)	**IPA** (ε = 17.9)
$E_{\text{stacked dimers}}$ **/ kJ mol^{-1}**	*p*PENTYLBA$_{St1}$	-33.0	-27.8
	*p*PENTYLBA$_{St2}$	-34.0	-31.5
	*p*PENTYLBA$_{St3}$	-37.2	-34.8
	*p*PENTYLBA$_{St4}$	-26.4	-22.9
	*p*BOBA$_{T1}$	-36.0	-30.3
	*p*BOBA $_{T2}$	-46.7	-38.4
	*p*BOBA$_{St1}$	-50.4	-46.0
	*p*BOBA$_{St2}$	-34.4	-32.5
	*p*TA*	-29.4	-26.1
	BA*	-12.8	-10.8
$E_{\text{H-Bonded dimers}}$ **/ kJ mol^{-1}**	*p*PENTYLBA $_{Hdimer1}$	-78.5	-58.2

	*p*PENTYLBA Hdimer2	-79.0	-58.7
	*p*BOBA$_{Hdimer1}$	-79.1	-59.4
	*p*BOBA$_{Hdimer2}$	-79.5	-59.6
	*p*TA*	-78.9	-58.4
	BA*	-78.6	-57.8

S5. General Experimental protocols.

S5.1 Materials. *p*PENTYLBA, > 99% was purchased from Sigma-Aldrich Co. Ltd. and PBOBA > 99.5% from Flurochem Ltd. Toluene (TOL) ≥ 99.9% was purchased from Fisher Scientific Company LLC., acetonitrile (MeCN) ≥ 99.5% from Sigma-Aldrich Co. Ltd., and isopropanol (IPA) ≥ 99.5% from Acros Organics. Of these all were used without further purification with the exception of *p*BOBA, which was recrystallized from toluene before use to remove occasional haziness apparent in some solutions prepared from as-purchased materials.

S5.2 Induction time measurements using the Crystal16™

The methodology is described fully in reference 13, we provide here a brief summary. The induction time measurements of the respective substituted benzoic acids (*p*PBOBA, *p*PENTYLBA) in different solvents (toluene, isopropanol) at 20 ^{0}C were determined as follows. Firstly a parent solution of 100 mL for *p*BOBA and 30 mL for *p*PENTYLBA was prepared by dissolving the desired amount of crystalline solid in the solvent for each targeted supersaturation. Using a micropipette 1.5 mL aliquots of this solution were distributed into each of the 16 vials. After that, the vial was quickly closed with a screw cap followed by wrapping with Parafilm. This combination of approaches aims to prevent solvent evaporation in order to maintain the desired concentration (i.e. supersaturation) of the solution over an extended time period of a few hours. The total weight of each sealed vial was measured on an analytical balance individually before placing the vials in the Crystal16™ equipment. Weights were checked after experiments to exclude those where evaporation may have occurred.
Subsequently, a temperature profile was custom designed for performing the induction time measurements and operated by the Crystal16™ equipment. Firstly the temperature was ramped to 40 ^{0}C at a rate of 5 ^{0}C min^{-1} and held for an hour to ensure complete dissolution of the crystalline solid in the solvent. Supersaturation was then generated by crash cooling the

solution at a rate of 5 ^{0}C min^{-1} to the desired operating temperature of 20 ^{0}C. It was held at that temperature for 8 hours. This was repeated five times to obtain (where possible) a number of 80 induction times at each individual supersaturation.

S5.3 Checking nucleated forms: PXRD results for *p*BOBA and *p*PENTYLBA

In the case of PENTYLBA no crystal structure was available in the CSD and so, as part of this study crystals, of 0.1 – 0.4 mm were grown from toluene through solvent evaporation and their structure determined at ambient conditions (Oxford Xcaliber 2 diffractometer, monochromatic Mo Kα radiation of wavelength, λ = 0.71073 Å with a graphite monochromator). As-purchased materials and the products of the nucleation experiments (ex Crystal16) were characterised using DSC and pXRD.

Figure S5.1: Crystal16^{TM} experiments PXRDs of samples of (a) *p*BOBA and (b) *p*PENTYLBA. Upper trace: Crystallised materials from Crystal16^{TM} experiment, middle trace: Sample bottle and bottom trace: Calculated CSD Ref.code (a) BUXBZA01 and (b) CCDC Deposition number 2003448.

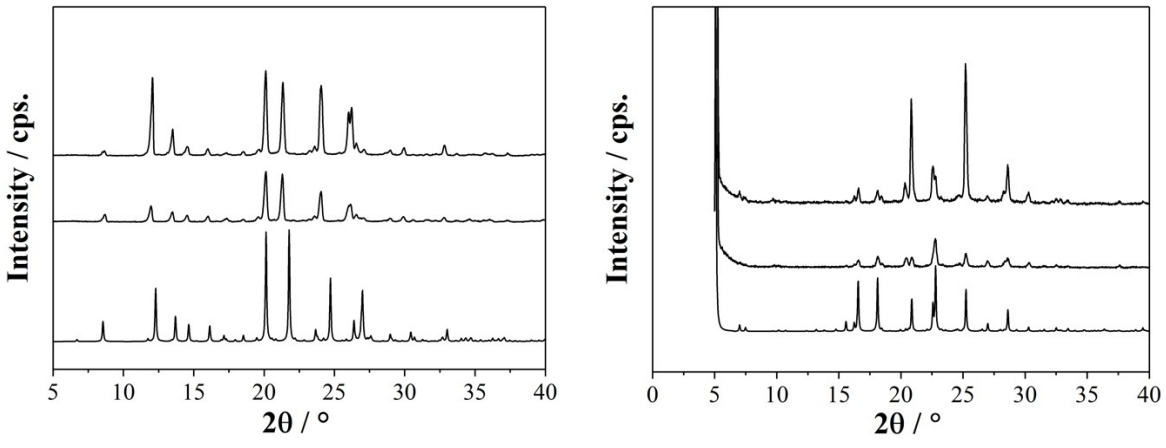

(a) (b)

References.

1. 'The Cambridge structural database' C. R. Groom, I. J. Bruno, M. P. Lightfoot and S. C. Ward, *Acta Crystallographica Section B: Structural Science, Crystal Engineering and Materials,* 2016, **72**, 171-179.

2. 'Mercury CSD 2.0–new features for the visualization and investigation of crystal structures' C. F. Macrae, I. J. Bruno, J. A. Chisholm, P. R. Edgington, P. McCabe, E. Pidcock, L. Rodriguez-Monge. R. Taylor, J. Van De Streek and P. A. Wood,. *Journal of Applied Crystallography*, 2008, **41**, 466-470.

3. 'Retrieval of Crystallographically-Derived Molecular Geometry Information' I. J. Bruno, J. C. Cole, M. Kessler, J. Luo, W. D. S. Motherwell, L. H. Purkis, B. R. Smith, R. Taylor, R. I. Cooper, S. E. Harris and A. G. Orpen, *J. Chem. Inf. Comput. Sci.*, 2004, **44**, 2133-2144.

4. 'Molecular and crystal structure of 4-alkoxybenzoic acids: Design of the mesogenic phase' L.G. Kuz'mina, N.S. Kucherepa, S.M. Pectov, A.N. Kochetov, N.S. Rukk and S.A.Syrby, *Kristallografiya*, 2009, **54**, 908-925.

5. Avogadro: an open-source molecular builder and visualization tool. Version 1.2.0 http://avogadro.cc/

6. 'Avogadro: An advanced semantic chemical editor, visualization, and analysis platform' M. D. Hanwell, D. E Curtis, D. C Lonie, T. Vandermeersch, E. Zurek and G. R. Hutchison; *J. Cheminformatics* 2012, **4**, 17.

7. Gaussian 09, Revision A.02, M. J. Frisch, G. W. Trucks, H. B. Schlegel, G. E. Scuseria, M. A. Robb, J. R. Cheeseman, G. Scalmani, V. Barone, G. A. Petersson, H. Nakatsuji, X. Li, M. Caricato, A. Marenich, J. Bloino, B. G. Janesko, R. Gomperts, B. Mennucci, H. P. Hratchian, J. V. Ortiz, A. F. Izmaylov, J. L. Sonnenberg, D. Williams-Young, F. Ding, F. Lipparini, F. Egidi, J. Goings, B. Peng, A. Petrone, T. Henderson, D. Ranasinghe, V. G. Zakrzewski, J. Gao, N. Rega, G. Zheng, W. Liang, M. Hada, M. Ehara, K. Toyota, R. Fukuda, J. Hasegawa, M. Ishida, T. Nakajima, Y. Honda, O. Kitao, H. Nakai, T. Vreven, K. Throssell, J. A. Montgomery, Jr., J. E. Peralta, F. Ogliaro, M. Bearpark, J. J. Heyd, E. Brothers, K. N. Kudin, V. N. Staroverov, T. Keith, R. Kobayashi, J. Normand, K. Raghavachari, A. Rendell, J. C. Burant, S. S. Iyengar, J. Tomasi, M. Cossi, J. M. Millam, M. Klene, C. Adamo, R. Cammi, J. W. Ochterski, R. L. Martin, K. Morokuma, O. Farkas, J. B. Foresman, and D. J. Fox, Gaussian, Inc., Wallingford CT, 2016.

8. ‘The M06 suite of density functionals for main group thermochemistry, thermochemical kinetics, noncovalent interactions, excited states, and transition elements: two new functionals and systematic testing of four M06-class functionals and 12 other functionals’ Y. Zhao and D. G. Truhlar, *Theoretical Chemistry Accounts*, 2008, **120**, 215-241.

9. ‘Universal solvation model based on solute electron density and a continuum model of the solvent defined by the bulk dielectric constant and atomic surface tensions’ A. V. Marenich, C. J. Cramer, and D. G. Truhlar, *J. Phys. Chem. B*, 2009, **113**, 6378-96.

10. ‘Effect of the Molecular Orientation on the Stability of Hydrogen-Bonded Benzoic Acid Dimers. Infrared Study of Liquid-Crystalline 4-Alkylbenzoic Acids.’, K. Takashi, J. Chihiro, K. Fumiko, U. Toshiyuki, U., *Bull. Chem. Soc. Jpn*., 1993, **66**, 3581-3584.

11. ‘Nucleation of Organic Crystals – A Molecular Perspective’, R. J. Davey, S. M. L. Schroeder, and J. H. ter Horst, Angew. Chem. Int. Ed. 2013, **52**, 2166-2179.

12. ‘Quantifying the Inherent Uncertainty Associated with Nucleation Rates Estimated from Induction Time Data Measured in Small Volumes.’, Y. Xiao, S. K. Tang, H. Hao, R. J. Davey and T. Vetter, *Cryst. Growth Des.* 2017, **17**, 2852−2863.

13. ‘Aromatic stacking - a key step in nucleation’. A. J. Cruz-Cabeza, R. J. Davey, S. S. Sachithananthan, R. Smith, S. K. Tang, T. Vetter, T and Y. Xiao, *Chem. Commun*. 2017, **53**, 7905−7908.

14. ‘*Ab initio* molecular dynamics for open-shell transition metals’ G. Kresse and J. Hafner, *Phys. Rev. B* 1993, **48**, 13115–13118;

15. ‘*Ab initio* molecular-dynamics simulation of the liquid-metal–amorphous-semiconductor transition in germanium’ G. Kresse and J. Hafner, *Phys. Rev. B* 1994, 49, 14251–14269;

16. ‘Efficiency of ab-initio total energy calculations for metals and semiconductors using a plane-wave basis set.’ G. Kresse, and J. Furthmüller, *Comput. Mater. Sci.* 1996, **6**, 15–50;

17. ‘Efficient iterative schemes for ab initio total-energy calculations using a plane-wave basis set.’ G. Kresse, and J. Furthmüller, J. *Phys. Rev. B - Condens. Matter Mater. Phys.* 1996, **54**, 11169–11186.

18. ‘Generalized gradient approximation made simple’ J. Perdew, K. Burke and M. Ernzerhof, *Phys. Rev. Lett*. 1996, **77**, 3865.

19. ‘Projector augmented-wave method’ P. Blöchi, *Phys. Rev. B* 1994, **50**, 17953;

20. ‘From ultrasoft pseudopotentials to the projector augmented-wave method.’ G. Kresse and D. Joubert, *Phys. Rev. B* 1999, **59**, 1758.

21. ‘Semiempirical gga-type density functional constructed with a long-range dispersion correction.’ S. J. Grimme, *Comput. Chem.* 2006, **27,** 1787–1799.

22. Implicit solvation model for density-functional study of nanocrystal surfaces and reaction pathways.’ K. Mathew, R. Sundararaman, K. Letchworth-Weaver, T. Arias, and R. Hennig, *J. Chem. Phys*. 2014 **140**, 084106.

23. ‘Implicit self-consistent description of electrolyte in plane-wave density functional theory.’ K. Mathew and R. Hennig, *J. Chem. Phys.* 2019 **151**, 234101.